

Magnetic and thermal properties of dysprosium aluminum garnet. III. Multiaxis phase transitions

D. P. Landau

Hammond Laboratory, Yale University, New Haven, Connecticut 06520
and Department of Physics and Astronomy*, University of Georgia, Athens, Georgia 30602

B. E. Keen†

Department of Engineering and Applied Science, Yale University, New Haven, Connecticut 06520

(Received 14 August 1978)

Dysprosium aluminum garnet is a cubic antiferromagnet with highly anisotropic moments along $\pm x$, $\pm y$, and $\pm z$ directions. In weak magnetic fields applied along any direction the zero-field antiferromagnetic state is stable. In strong magnetic fields, of the order of 10 kOe, applied along [110] or [001], those spins with a component along the field are driven paramagnetic. Because of the unusual symmetry of the magnetic lattice, the remaining (transverse) spins are decoupled from the others and are ordered at low temperatures by their own spin-spin interactions. We have investigated the magnetic phase diagrams with fields along [110] and [001] by making specific-heat and susceptibility measurements from 0.4 to 4.2 K in applied magnetic fields as large as 15 kOe. Specific-heat measurements were also made for fields slightly misaligned from [001], and the entire (110) plane was studied by adiabatic field rotation. The phase boundaries separating the simple antiferromagnetic and paramagnetic states contain tricritical points; the first-order portion of the phase boundary and the associated latent heat were measured by isothermal demagnetizations and magnetizations. We have analyzed the data to extract the critical fields and other characteristic parameters for both the simple antiferromagnetic phase as well as the "transverse" ordered states.

I. INTRODUCTION

In dysprosium aluminum garnet (DyAlG) the unusual symmetry of the crystal field produces different local anisotropy axes at different sites. As a result the magnetic ions are constrained to lie along one of the cubic axes (i.e., $\pm x$, $\pm y$, or $\pm z$),¹ and below 2.54 K the magnetic interactions produce an ordered-antiferromagnetic state with three pairs of sublattices as shown in Fig. 1(a). Each type of site also has "local" axes (x' , y' , z') for the g -tensor, and the local high- g_z direction may lie in the crystallographic x , y , or z directions. The application of a magnetic field in an arbitrary direction may then produce different effects at different sites. The cubic space group of DyAlG (O_h^{10}) retains the threefold symmetry about [111] in going to the magnetic system. Because of this symmetry, all of the sites with a component of the applied field, H_0 , along the spin direction become equivalent (e.g., for H_0 along [111], $+x$, $+y$, and $+z$ are equivalent as are $-x$, $-y$, and $-z$). In two previous papers^{3,4} we have considered this simple case and have reported the results of extensive magnetothermal measurements and the

analysis of the measured thermodynamical properties as well as the accompanying magnetic phase diagram. (In these papers we also show that below 4 K the system can be quite well described by a model of Ising-like $S' = \frac{1}{2}$ spins. The local z' axis of the effective spin varies with site as described above.) Several unusual features of the magnetic and thermal behavior, as well as the results of neutron scattering⁵ and magneto-optical experiments,⁶ were explained by Blume *et al.*⁵ who noted that the unusual symmetry in DyAlG permits a coupling between the antiferromagnetic order parameter and the *uniform* applied field. Application of the field thus simultaneously introduces an effective "staggered" field. The point at which the transition changes from first order to second order is thus a "wing" critical point.⁷ For certain special symmetry directions such as [001] and [110], this effect is not allowed⁵ and the observed behavior should be completely characteristic of a multiaxis Ising system in a uniform field. The application of a magnetic field along "special" directions other than [111] may then produce a transition from an antiferromagnetic configuration to the paramagnetic state (with the spins aligned along a $+z'$ local

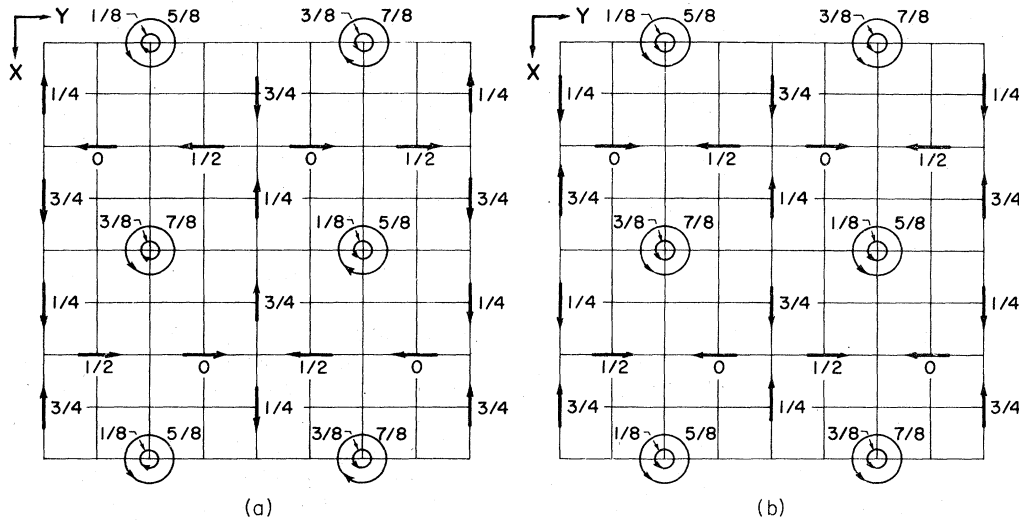


FIG. 1. (a) Zero-field antiferromagnetic-spin arrangement in dysprosium aluminum garnet, shown in a (001) plane projection of the unit cell. The numbers give the heights above the $Z=0$ plane. Spins pointing along the z axis are indicated as current loops in a right-hand sense (as in Ref. 2). (b) Proposed antiferromagnetic arrangement of the x and y spins when the z spins are aligned by a strong magnetic field along [001].

axis) for either one or two pairs of sublattices while the other sublattices may become disordered or undergo transitions to a new antiferromagnetic or even ferromagnetic state.⁸ Motizuki⁹ has considered similar multisublattice transitions in methylamine chrome alum in the molecular-field approximation; however, since this salt orders near 0.015 K,¹⁰ the different types of transitions with fields along various directions have not been studied. We believe then that the multiaxis phase transitions which are reported here are the first ones to be studied experimentally. (In Sec. II we shall see further that DyAlG is highly unusual in that perfectly aligned paramagnetic spins are completely decoupled from all spins which are perpendicular to them.) Preliminary accounts of some of this work may be found in Refs. 8, 11, and 12. Low-temperature magnetization measurements and interpretation with fields in the (110) plane have also been reported by Bidaux *et al.*¹³⁻¹⁶ Their experimental results are quite helpful although some of the analysis is not complete. We shall discuss their work more carefully in the next paper in this series.

In this paper we shall first indicate the kinds of effects which we might expect to observe and then report the results of extensive magnetothermal measurements made with fields along (or near) [110] and [001]. Effects due to slight misalignment of the applied magnetic field produce rather bothersome (but necessary) corrections in the analysis. These will be discussed where appropriate. We shall then extract a number of parameters which are characteristic of the system with fields in these directions. These parameters, along with some of those determined in Paper II, of this series (Ref. 4) will be used in the next pa-

per in this series in order to determine the spin-spin interaction constants.

II. BACKGROUND

A. Description of "multiaxis" transitions

Various ordered configurations have been considered as possible multiaxis ordered states in DyAlG.^{12,17} These states can be represented by three letter symbols, with P , A , or F denoting paramagnetic, antiferromagnetic or ferromagnetic order, respectively, at each type of site. An alphabetic subscript d is used to denote a disordered state and m a magnetized state. Inequivalent antiferromagnetic states are distinguished by the use of numerical subscripts (i.e., A_1, A_2, A_3 , etc.). Since there are three pairs of sublattices (corresponding to $\pm x$, $\pm y$, and $\pm z$ spins) we can describe all possible six-sublattice states by a triad of symbols. For example, the (P_d, P_d, P_d) state shown at the top of Fig. 2 is the high-temperature zero-field paramagnetic state in which all three sublattices are paramagnetic and disordered. With the application of a strong magnetic field along [111], all three sublattices become strongly magnetized and the magnetic state is denoted (P_m, P_m, P_m) . In the zero-field antiferromagnetic state, each of the three sublattices is ordered in one type of antiferromagnetic configuration, A_1 . In DyAlG, the (A_1, A_1, A_1) state corresponds to the ordering shown in Fig. 1(a).

For H_0 along [001] the field acts on only the $\pm z$ sublattices, and at a certain critical field $H_{[001]}^c(T)$ it

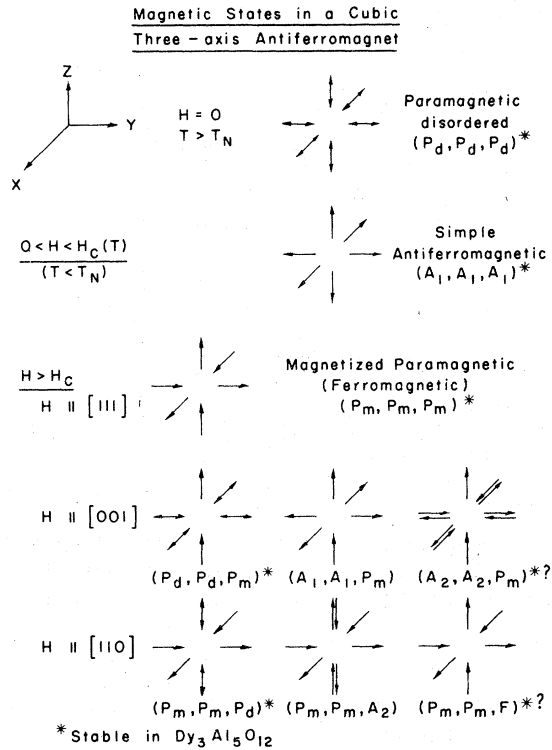


FIG. 2. Schematic representation of magnetic states in a cubic three-axis antiferromagnet. States which are believed to be stable in DyAlG are marked with a star.

will cause the $-z$ spins to reverse, as in the case of a single anisotropic sublattice pair. To first order the $\pm x, \pm y$ (transverse) spins are unaffected by the applied field H_0 , which is perpendicular to the local g_z , (and $g_x, g_y \sim 0$).⁴ When the z spins have undergone a transition to the completely magnetized paramagnetic state (P_m), their coupling to the transverse field is exactly zero. This is demonstrated in Fig. 3 for two of the nearest neighbors of a transverse spin. (The spin representation is the same as in Fig. 1.)

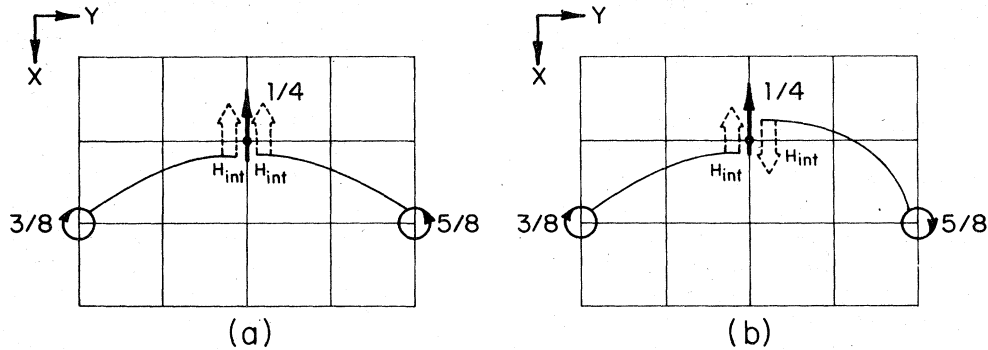


FIG. 3. Effect of the phase transition on nearest-neighbor interactions. The notation is the same as that used in Fig. 1: (a) in the simple antiferromagnetic states the interaction fields H_{int} due to two z spins add at an x -spin nearest-neighbor site, (b) with the two z spins aligned parallel, the interaction fields at the x -spin nearest neighbor cancel out. The same effect occurs at sites of spins directed in the $\pm y$ direction.

Of course when the paramagnetic spins are not completely aligned there will still be some short-range order coupling to the transverse spins, and we should expect to see manifestations of this in the thermodynamical behavior. When the applied field is much greater than the critical field $H_{[001]}^{\perp}(T)$, the z spins will thus be completely decoupled. Hence, the transverse spins will comprise a new system which will be paramagnetic at high temperatures and, at some sufficiently low temperature $T_{[001]}^{\perp}$, will undergo a cooperative phase transition. In this high-field ordered state, below $T_{[001]}^{\perp}$ the transverse spins may have the same orientation as they do in the simple zero-field antiferromagnetic state (A_1, A_1, P_m) or may form a completely new structure, e.g., (A_2, A_2, P_m). In Fig. 1 we show a (001) projection of both the zero-field antiferromagnetic spin arrangement in DyAlG and a particular, new antiferromagnetic arrangement of x and y spins (predicted on the basis of dipolar interactions) aligned by a field along [001]. The possible alternatives have been considered in detail¹¹ and will be discussed at length in the next paper in this series. Low-temperature ordered states were also considered by Bidaux *et al.*¹⁵ who used a different notation.

Treating the transition by simple molecular-field theory, we find that the low-field phase boundary to the simple antiferromagnetic state (A_1, A_1, A_1) should be parabolic,⁹ with the transition to the paramagnetic state (P_d, P_d, P_m) being second order near T_N . For lower temperatures, a tricritical point T_t could appear below which this transition would be first order (depending on the ratio of the intrasublattice interactions to the intersublattice coupling).

For $\vec{H} \parallel [110]$ the situation is superficially the same. Once again the transition from the antiferromagnetic to paramagnetic state could be first order below a tricritical point T_t and second order above T_t (up to $T = T_N$). At low temperatures we expect an order-order transition in which the transverse spins become magnetized paramagnetic due to the applied

field, and the $\pm z$ spins are cooperatively aligned by spin-spin interactions with other z -type spins. Again, due to the magnetic symmetry, the interaction fields produced by the transverse spins cancel identically, and chains of spins pointing in the $\pm z$ direction remain (see Fig. 1). The assumption of antiferromagnetic chains of z spins [as in the simple antiferromagnetic state shown in Fig. 1(a)] yields a positive internal energy U/R at $T=0$ K, i.e., the state is unstable, on the basis of dipolar interactions alone. In fact dipolar interactions predict the ordered state to be composed of ferromagnetic chains which are aligned in a three-dimensional ferromagnetic state, i.e., the state (P_m, P_m, F) .

B. Asymptotically exact theories

The effective interaction Hamiltonian for DyAlG has the form

$$\mathcal{H} = \sum_{i>j} K_{ij} \sigma_i \sigma_j + \frac{1}{2} \mu_B H \sum_i g_i \sigma_i, \quad (1)$$

where $\sigma_i, \sigma_j = \pm 1$ and g_i is the effective g value in the direction of the applied field H . The interaction parameters K_{ij} include both dipolar and nondipolar contributions, and their determination will be discussed in detail in Paper IV. It is nonetheless possible, using Eq. (1), to derive the general form for theoretical expressions for thermodynamical properties; these expressions become asymptotically exact for some limiting value of field and/or temperature.

$$C/R = (\Delta/kT) \exp(-\Delta/kT) \left[\frac{1}{2}(y + y^{-1}) + (\delta/\Delta)(y - y^{-1}) + (\delta/\Delta)^2 \frac{1}{2}(y + y^{-1}) \dots \right], \quad (3)$$

where we have $\delta = g \mu_B H$ and $y = \exp(\delta/kT)$.

In the presence of a strong magnetic field the spins will be paramagnetic and the specific heat will be a Schottky anomaly of the form

$$\frac{C}{R} = \left(\frac{\Delta}{kT} \right)^2 \frac{\exp(-\Delta/kT)}{[\exp(-\Delta/kT) + 1]^2}, \quad (4)$$

where we have $\Delta = g \mu_B (H_0 + h_i)$ and h_i is the effective spin-spin interaction field. In the present situation it is possible that, due to the field orientation, different sublattices will be in different states. For example, with H_0 along [001], the z spins will be paramagnetic and aligned, and the "transverse" spins will be antiferromagnetic. If the field is now slightly misaligned towards [011], a field component will be along the transverse-spin local g_z axis and Eq. (4) will therefore be applicable. (We shall see later that

These expressions will contain certain "characteristic parameters" which are simply related to the interaction parameters K_{ij} . As this has been examined at length in Ref. 4, we shall not derive all the formulas but shall present them and show in particular how they apply to the more complicated "multisublattice" nature of the present results.

In such a highly anisotropic system the low-temperature elementary excitations are single ion "spin flips" rather than collective excitations. It is straightforward to determine the low-temperature thermodynamical behavior in terms of the energies of the elementary excitations and their relative probabilities. At very low temperatures where only single spin-flip excitations of energy Δ are important the resultant specific heat is

$$C/R = (\Delta/kT)^2 \exp(-\Delta/kT). \quad (2)$$

As the temperature increases and contributions from higher-lying excitations become important, Eq. (2) becomes insufficient although it is still possible to empirically fit the data to the same form using an "effective" splitting Δ_{eff} , which approaches Δ at $T \rightarrow 0$. With the application of a small magnetic field the form of the specific heat depends upon the nature of the ground state. If the zero-field ordered state is ferromagnetic, Eq. (2) remains correct but Δ is replaced by $\Delta + g \mu_B H$. However, if the ground state is antiferromagnetic, the energies of single spin-flip excitations are different for spins which were originally up and those which were down. The low-temperature specific heat is then^{11,18}

misalignment effects are very important.)

The effect of the small (but finite) g_{\perp} is also of concern. The excitation energy for the transverse spins due to an applied field H_0 which is misaligned from the [001] direction by an angle θ is

$$\Delta = \mu_B [g_{\parallel}^2 (H_0 \sin \theta + h_i)^2 + g_{\perp}^2 H_0^2 \cos^2 \theta]^{1/2}, \quad (5)$$

where h_i is the effective spin-spin interaction field. The ratio of the terms involving the misalignment and g_{\perp} is

$$R = (g_{\parallel}/g_{\perp})^2 (2h_i \sin \theta / H_0 \cos^2 \theta) \approx 100 \quad (6)$$

for $\theta \sim 2^\circ$. Misalignment effects will then dominate the effects of g_{\perp} .

At high temperatures an expansion of the partition function yields a specific heat whose temperature dependence is given by

$$C/R = \Theta_2/2T^2 + \Theta_3/3T^3 + \dots, \quad (7)$$

where

$$\Theta_2 = \frac{1}{k^2} \sum_j K_{jj}^2, \quad \Theta_3 = \frac{6}{k^3} \sum_{j>k} K_{jj} K_{jk} K_{ki}.$$

In the presence of a small magnetic field, Eq. (7) will include terms like $\lambda H_0^2/RT^2$, where λ is the Curie constant.

At $T=0$ the application of a sufficiently strong magnetic field H^c will produce a phase transition when the energy of the high-field state becomes equal to that of the zero-field state, i.e.,

$$M_0 H^c = U_{H=0} - U_{H_0}, \quad (8)$$

where M_0 is the magnetization of the high-field state, and $U_{H=0}$ and U_{H_0} are the internal energies of the zero-field and high-field states, respectively. Since these are determined by the interactions (K_{ij}), the critical field H^c will provide a direct measure of the interaction "bonds" which change during the transition.

III. EXPERIMENTAL METHODS

The apparatus used for these experiments, as well as the techniques used, were explained in detail in a previous paper³ and will be discussed only briefly here. A large single-crystal ellipsoid of DyAlG was supported in the cryostat with a (110) plane horizontal. This plane contained the minor axes of the ellipsoid, and the classical demagnetizing factor in this plane was $N = 5.35$. The sample could be cooled to 0.4 K with a He³ cryostat surrounded by a He⁴ bath. Magnetic fields up to 15 kOe were supplied by an electromagnet which could be rotated so that the field could be aligned along any direction in the (110) plane. The location of the [001], [111], and [110] axes was deduced from the results of adiabatic field rotations. (This method was described more fully in Ref. 3.) The specific heat of the sample was measured in magnetic fields up to 15 kOe and at temperatures between 0.4 and 4.2 K, using the standard-heat pulse method.³ Values obtained for the specific heat are accurate to better than $\pm 2\%$. The data were corrected for contributions from the addendum, the lattice, and the hyperfine interactions as described in Refs. 3 and 4. The results reported here are the net resultant values for the (electronic) magnetic specific heat. A far more important source of error in these measurements is the determination of the actual orientation of the applied magnetic field. Above 1.1 K, the only stable orientation of the magnetic field, with respect to creation of a torque due to the field not being parallel to the moment, is [111].¹⁹ This means that the application of a magnetic field near

[110] or [001] (but not exactly along these axes) will tend to rotate the entire sample so that the [111] axis would be parallel to the field. The resultant torque was sufficiently great to shatter several sample supports ($\frac{1}{4}$ -in.-phenolic tubing). The effects of this misorientation will be discussed at length in Sec. IV. At low temperatures any misalignment of the field will produce a component of the field parallel to those spins which are ostensibly in a zero-field state (i.e., the local g_z is perpendicular to H_0). The form for the low-temperature specific heat will then be changed, and this too will be discussed in Sec. IV.

For at least one set of experiments we wanted to insure that the sample support was absolutely rigid. This rigidity was achieved by using an 8-cm length of $\frac{1}{4}$ -in.-o.d. stainless-steel tubing (0.010-in. wall thickness) as a support. The heat leak with respect to the sample with this support was quite large (as much as 10–20 ergs/sec), and it was impossible to use our standard-heat pulse technique for specific-heat measurements. Instead we adopted the continuous heating technique (see Refs. 20 and 21 for details concerning this technique). Heating rates were typically 500 ergs/sec although very near the transition rates as small as 100 ergs/sec were used. These heating rates were far too large to allow high-resolution measurements to be made, but were quite reasonable for allowing us to determine the location of the transition temperature to ± 5 mk and the maximum value of the specific heat to $\pm 10\%$. An additional series of adiabatic rotations showed no evidence of sample rotation even in fields of 12 kOe and at temperatures as low as 0.6 K. The torque produced under these conditions was calculated to be almost a factor of 2 larger than those which had caused previous sample supports to shatter.

Isothermal-field sweeps were made by varying the field such that the magnetocaloric effect caused the sample to cool and then, by supplying heat electrically through a feedback loop, keeping the sample temperature constant. The heat supplied Q was measured as a function of field, thus allowing us to determine

$$(\partial S/\partial H_0)_T = (1/T)(\partial Q/\partial H_0)_T$$

to $\pm 5\%$. The technique was described in Ref. 3.

Susceptibilities were measured by observing the change of mutual inductance of a pair of astatic coils with the sample centered in one of the secondaries. Measurements were also made in the presence of a magnetic field aligned perpendicular to the coil axis. Changes in mutual inductance were made in part using a Hartshorn bridge²² and in part by phase locking onto the inductive component of the signal from the secondary using a PAR HR8 lock-in detector. In order to measure the susceptibility along a [001] direction with the large static field along [110], it was

necessary to support the sample at 90° to the configuration described above. The sample was first oriented by Laue backreflection x-ray patterns to have the [001] axis vertical and then encased in a Teflon sample holder. It was estimated that the sample was actually within $\pm 5^\circ$ of the desired orientation when in situ. As we shall see, the question of orientation near [001] is quite important. In all cases the measured mutual inductance included a constant contribution from the cryostat. This contribution was removed by normalizing the high-temperature results to the known form of the high-temperature susceptibility plus a constant. This procedure also served to establish an absolute scale for the susceptibility of the sample.

IV. EXPERIMENTAL MEASUREMENTS: RESULTS

A. Thermal measurements with applied fields along [001]

1. Specific-heat measurements

Specific-heat measurements were made in constant applied fields from 1 to 15 kOe at temperatures between 0.5 and 4.2 K. A variety of results were obtained and typical data are shown in Fig. 4. Preliminary results have already been presented in Ref. 8. For relatively small fields, single sharp peaks were observed whose height decreased as the applied field was increased.²³ For fields between 5.8 and 7.0 kOe a sharp low-temperature peak appeared followed by a broader less prominent peak at higher temperatures. For fields above 7 kOe only a single very sharp peak was present; these λ -like peaks showed rather anomalous behavior as a function of increasing field. We shall discuss the results in more detail later. The various specific-heat maxima were taken to indicate phase transitions whose locations are plotted in the magnetic phase diagram shown in Fig. 5. It would, of course, be desirable to show curves of the shape-independent specific heat at constant *internal* field C_{H_i} ; however, we lack the extensive information about the magnetization derivatives which is needed in order to correct C_{H_0} to C_{H_i} . (See Refs. 3 and 25 for discussion of the complex relation between the two quantities). The location of the phase boundaries was also carried out by making a series of isothermal field sweeps as described in Sec. III. The data indicate that for

$$1.65 \text{ K} \lesssim T < T_N (=2.53 \text{ K})$$

the transition to the paramagnetic state [i.e., $(A_1, A_1, A_1) \rightarrow (P_d, P_d, P_m)$] is of second (or higher) order. These two phases are shown schematically in Fig. 2. The data also suggest that a tricritical point

occurs at $T_i \sim 1.65 \text{ K}$ ($H_{0i} \sim 5.30 \text{ kOe}$) below which the transition is of first order. (More recent measurements²⁶ made with a carefully aligned sample and very high resolution suggest that the discontinuity in the magnetization approaches zero linearly with temperature and that the value of T_i with the field perfectly aligned is 1.80 K.) The tricritical temperature is almost exactly the same as the temperature for which the first-order transition with $\vec{H}_0 \parallel [111]$ appears.^{3,27,28} The first-order transition below T_i is spread out into a coexistence region due to the demagnetizing field in a sample with finite-demagnetizing factor N . In this mixed phase region the (A_1, A_1, A_1) and (P_d, P_d, P_m) phases coexist. (For $\vec{H}_0 \parallel [111]$ the field affects all three pairs of sublattices equally and the coexistence region consists of a mixture of (P_m, P_m, P_m) and (A_1, A_1, A_1) .³) At low temperatures the application of a strong magnetic field produces the (A_2, A_2, P_m) state. Previous ground-state calculations^{8,11} using dipolar coupling only have predicted that this rather unusual transition should include the appearance of an antiferromagnetic-ordered state in the two sublattices which are perpendicular to the applied field. Preliminary neutron scattering results²⁹ tentatively confirm this. Due to the demagnetizing field this transition is also spread out into a coexistence region combining (A_1, A_1, A_1) and (A_2, A_2, P_m) . This transition is bounded above and below by fields H_0^+ and H_0^- given by

$$H_0^\pm = H_i^c + NM^\pm, \quad (9)$$

where H_i^c is the critical-internal field and M^+ and M^- correspond to the upper and lower values of the magnetization at the transition. The sharp transition which was found at $\sim 1 \text{ K}$ with $H_0 \leq 7 \text{ kOe}$ indicates the transition between two different sets of mixed, coexisting phases

$$(A_1, A_1, A_1) + (A_2, A_2, P_m) \rightarrow (A_1, A_1, A_1) + (P_d, P_d, P_m).$$

For $H_0 \geq 7 \text{ kOe}$ the almost vertical phase line beginning at $T_N' = 1.01 \text{ K}$ shows the transition from the (transverse) ordered multisublattice state (A_2, A_2, P_m) to the paramagnetic (P_d, P_d, P_m) phase. Just above H_0^+ the specific-heat anomaly was quite sharp but not particularly large. As the value of the applied field was raised, the maximum increased in magnitude and moved first to higher and then to lower temperature. The initial increase in $T_{[001]}^+$ was almost certainly caused by the proximity to the mixed phase region and short-range order in the z spins. We believe that the bending back of $T_{[001]}^+$ at high fields is due to a small misalignment of the applied field with respect to the [001] axis. In order to test for this possibility we made a detailed study of this upper-phase arm for fields applied at several different angles with respect to [001]. The resultant-phase boundaries are plotted in Fig. 6.

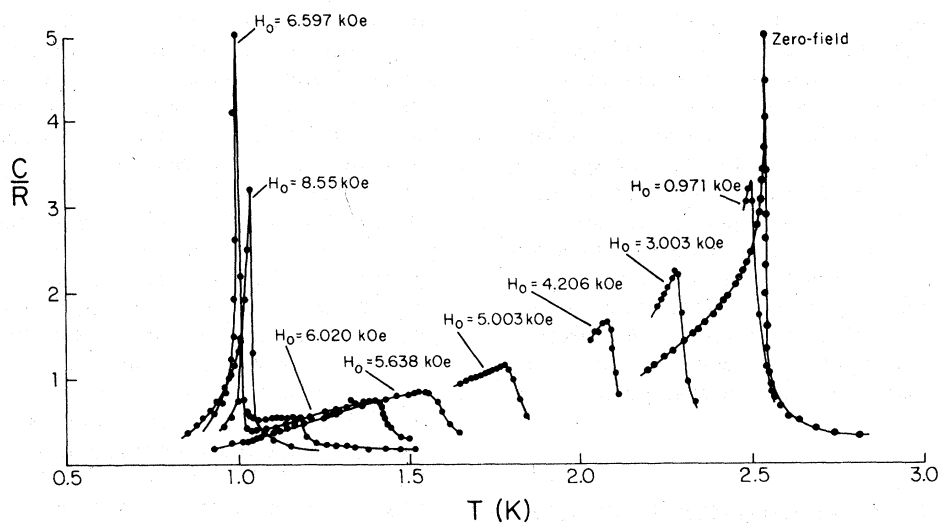


FIG. 4. Specific heat of DyAlG with applied magnetic fields along [001]. The peaks found above 1.65 K correspond to the transition $(A_1, A_1, A_1) \rightarrow (P_d, P_d, P_m)$. (See Fig. 2). Between 1.1 and 1.65 K the transitions are $(A_1, A_1, A_1) + (P_d, P_d, P_m) \rightarrow (P_d, P_d, P_m)$. Transitions below 1.1 K and fields less than 7.1 kOe are $(A_1, A_1, A_1) + (A_2, A_2, P_m) \rightarrow (A_1, A_1, A_1) + (P_d, P_d, P_m)$. The peak in the 8.55 kOe curve indicates a transition of $(A_2, A_2, P_m) \rightarrow (P_d, P_d, P_m)$.

In several sets of experiments the peak value of the specific heat became quite large ($C/R_{\max} \geq 5$) at $T_{[001]}$ for applied fields on the order of 10 kOe or above. (We now believe that in these cases the field

was actually misaligned by the order of 2° , and the unusual phenomenon which we shall now describe further emphasizes the importance of correct alignment in studying the multisublattice transitions.)

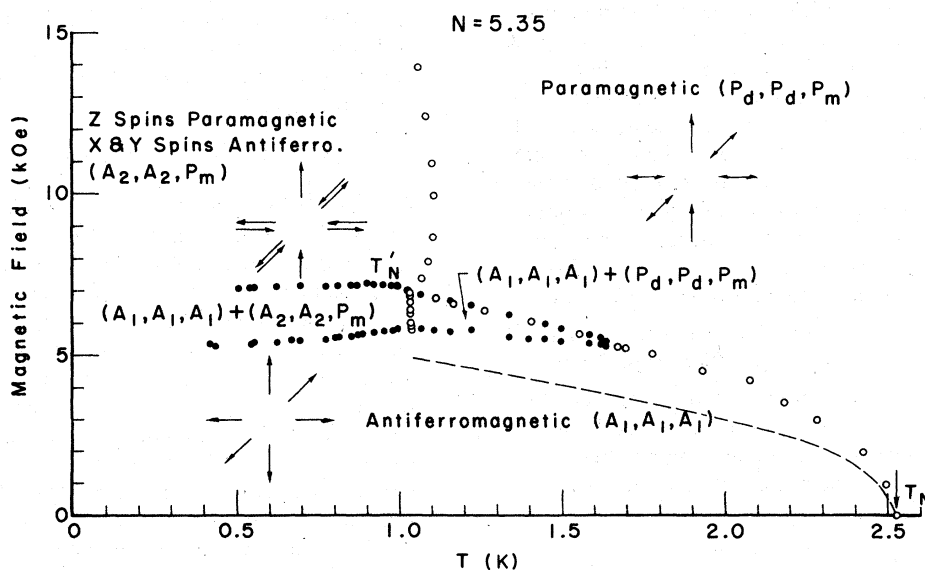


FIG. 5. Magnetic phase diagram for DyAlG with applied magnetic fields along [001]: open circles are the maxima of C_{H_0} vs T curves such as those shown in Fig. 4, and closed circles are the end points of first-order transitions determined from isothermal field sweeps. The broken line is the phase boundary calculated from the experimental data of Wyatt (Ref. 24) for the case of $N=0$.

When the field was increased to 12 kOe or above, the specific heat actually became *negative* at the critical temperature. The effect was clear and reproducible: during a heating interval the sample would begin to cool. When the heating stopped the sample temperature reached equilibrium rather quickly but then cooled further when the heat was turned on again. Eventually the sample temperature began to increase when the heat was applied. The total amount of energy involved varied with field magnitude and orientation but was about $0.04R$ or less in all cases. Four different runs made with the field orientation fixed are shown in Fig. 7. An explanation of this anomalous behavior will be given in Sec. V A 2.

2. Latent-heat measurements

The latent heat associated with the first-order portion of the critical-field curve was examined by means of isothermal-field sweeps, and the result is shown in Fig. 8. The unusual characteristic of these results is that below 0.9 K the latent heat becomes negative. A positive latent heat means that heat

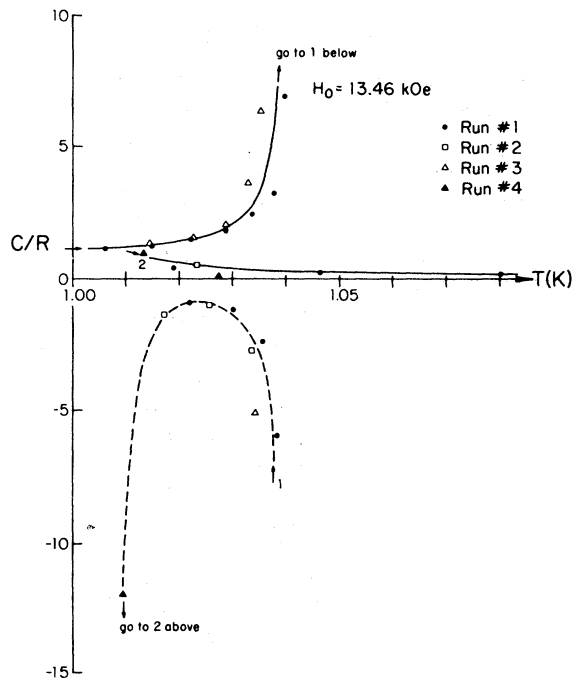


FIG. 7. Apparent "negative" specific heat of DyAlG with 13.46 kOe slightly misaligned from the [001] direction.

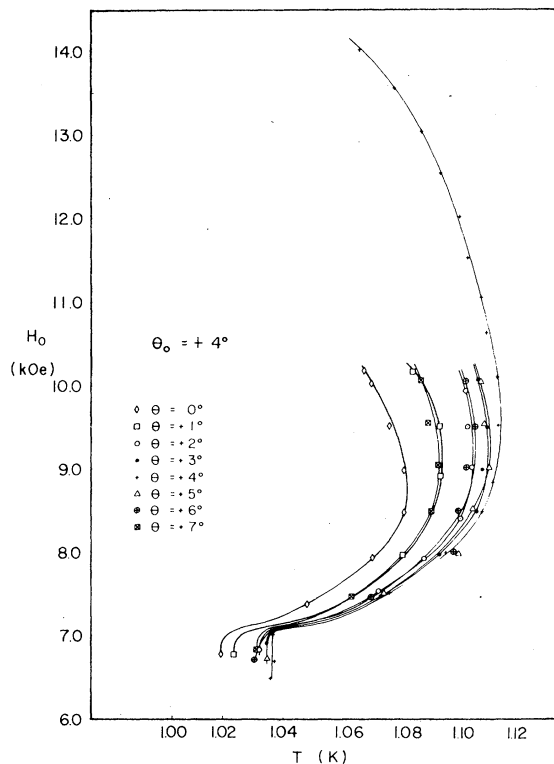


FIG. 6. Dependence of low-temperature high-field boundary in DyAlG with direction of the field near [001]. θ is measured with respect to the magnet and therefore, bears no relation to crystal axes.

must be supplied to convert the antiferromagnetic state to the disordered phase. From the magnetic Clausius-Clayperon equation

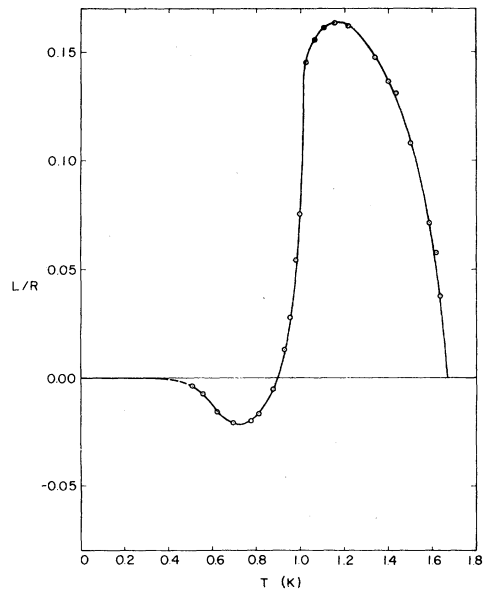


FIG. 8. Experimentally measured latent heat in DyAlG associated with the first-order phase transition in magnetic fields along [001].

$$L(T) = -T[M^+(T) - M^-(T)] \frac{\partial H_f^c(T)}{\partial T}, \quad (10)$$

we see that this implies $\partial H_f^c/\partial T > 0$ although there is no magnetization data from which the latent heat can be calculated. However, by 0.5 K the latent heat is essentially zero, indicating that $H_{[001]}^c(T \rightarrow 0)$ has zero slope (see Fig. 5). The dashed portion of the curve shows a reasonable extrapolation of the data in the region of temperature for which irreversible effects make measurements impossible.

Adiabatic-field sweeps show irreversible effects caused by entering the mixed phase. Similar irreversibilities had been found when we have $\vec{H}_0 \parallel [111]$, in which case a comparison with the entropy-temperature curves derived from the integrated specific heat showed the effect on the isothermal-latent-heat measurements, was somewhat less than on the adiabatic-field sweeps.³ Based on these results and less extensive measurements in the [001] direction, it appears likely then, that the latent-heat curve shown in Fig. 8 is correct to within an error in entropy ΔS of $0.02R$ where $L = T\Delta S$.

B. Thermal measurements with applied fields along [110]

1. Specific-heat measurements

The specific heat of DyAlG with fields up to 12 kOe along the [110] axis was measured down to 0.4 K. The results (see Fig. 9) are quite similar to those

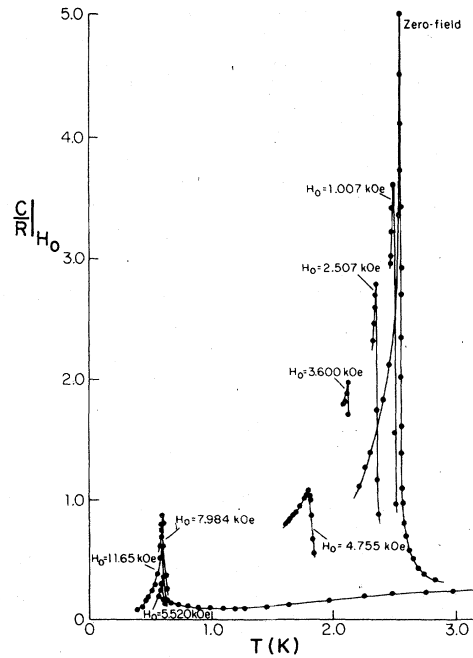


FIG. 9. Specific heat of DyAlG with applied magnetic fields along [110]. The transitions above 1.6 K are $(A_1, A_1, A_1) \rightarrow (P_m, P_m, P_d)$ (see Fig. 11). The transition at 0.6 K for $H_0 = 5.52$ kOe is $(A_1, A_1, A_1) + (P_m, P_m, F) \rightarrow (A_1, A_1, A_1) + (P_m, P_m, P_d)$ and for fields above 7.5 kOe are $(P_m, P_m, F) \rightarrow (P_m, P_m, P_d)$.

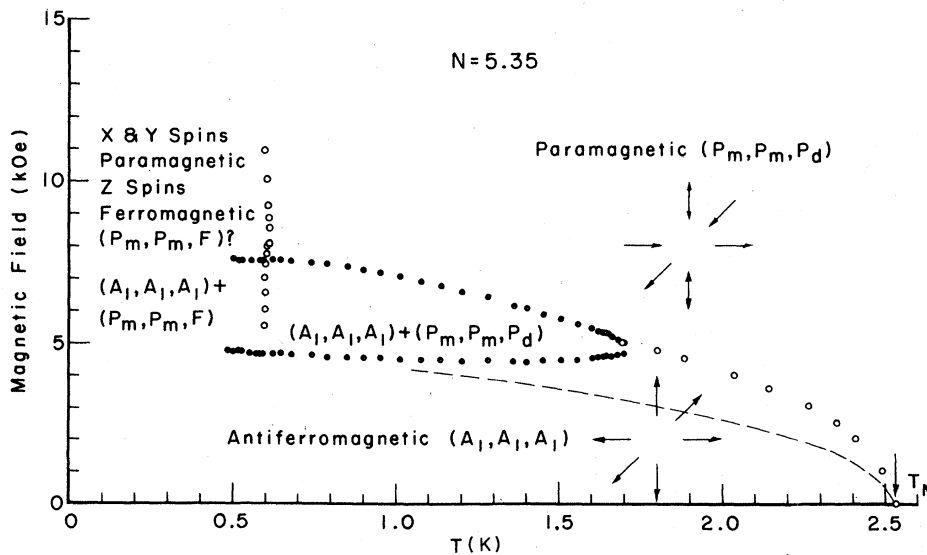


FIG. 10. Magnetic phase diagram for DyAlG with applied magnetic fields along [110]: open circles are the maxima of C_{H_0} vs T curves such as those shown in Fig. 9, and closed circles are the end points of first-order transitions determined from isothermal field sweeps. The broken line is the phase boundary calculated from the experimental data of Wyatt (Ref. 24) for the case $N=0$.

found for the [001] case. Again the specific heat showed relatively sharp peaks, and the phase boundary traced out by the specific-heat maxima and latent-heat measurements is shown in Fig. 10. The low-field transition from the simple antiferromagnetic state is to the (P_m, P_m, P_d) state, whereas the low-temperature high-field state is (P_m, P_m, F) (see Fig. 2). The specific-heat peaks encountered upon crossing the vertical phase boundary at $T'_{[110]}$ were quite sharp, although the maximum values were much smaller than the equivalent [001] values. The curvature of the upper-phase arm is appreciably less than for $\vec{H} \parallel [001]$. The insensitivity of the specific heat to the magnitude of the applied field (for $H_0 > 8$ kOe) is shown in Fig. 11.

2. Latent-heat measurements

The latent heat associated with the first-order phase transition was measured in an identical manner as for the [111] and [001] cases. The results of these measurements are shown in Fig. 12. Here, too, the rather abrupt decrease of the latent heat at low temperatures is probably due to irreversibilities (with an associated change in entropy as $\Delta S \leq 0.02R$) and the dashed line shows a reasonable extrapolation to $T=0$.

C. Adiabatic-field rotation with H_0 in the (110) plane

An independent check on the thermal properties with fields along (or near) [001] and [110] is provided by placing a field along [111], where the entropy

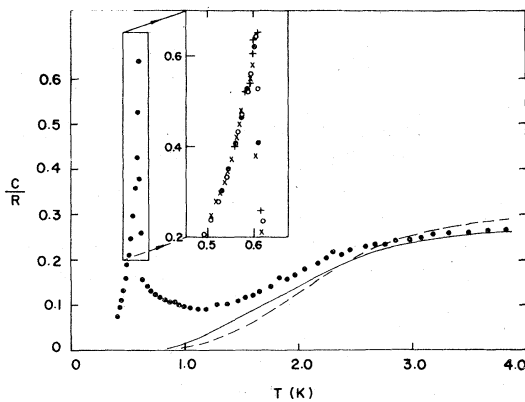


FIG. 11. Specific heat of DyAlG with 11.6 kOe along the [110] direction. The dashed line shows a Schottky specific-heat curve for the transverse spins. The solid curve shows a Schottky curve for the transverse spins modified by the effects of short-range order in the "parallel" spins. High-resolution insert data: (+) $H_0=8.860$ kOe, (●) $H_0=9.051$ kOe, (○) $H_0=10.227$ kOe, (x) $H_0=11.945$ kOe.

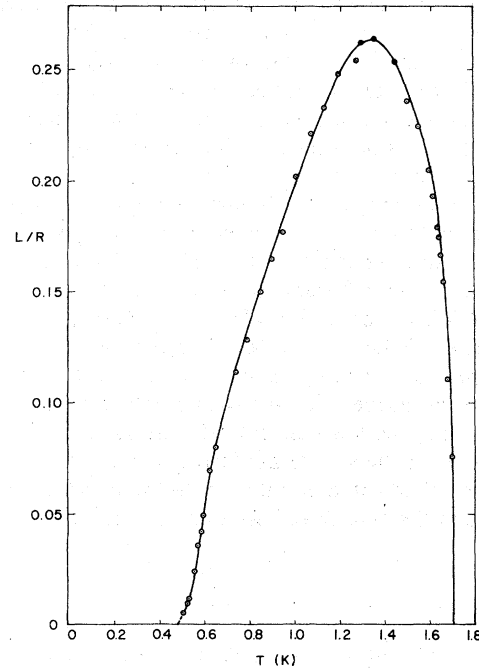


FIG. 12. Experimentally measured latent heat for DyAlG associated with the first-order phase transition in fields along [110].

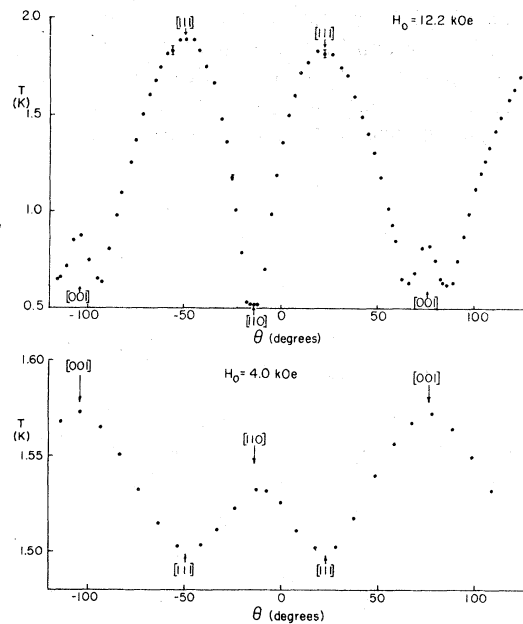


FIG. 13. Adiabatic-field rotations in DyAlG: (a) Variation of temperature with angle with $H_0=12.2$ kOe. $S/R=0.054$ for H_0 along [111] and $T=1.88$ K. (b) Variation of temperature with angle for $H_0=4.0$ kOe; $S/R=0.185$ and $T=1.50$ K.

and energy characteristics are known,³ and rotating the field adiabatically to other positions. Previous measurements^{3,30} had shown that the magnetocaloric effect is quite big in DyAlG. We have studied this effect in detail by carrying out a series of adiabatic-field rotations for various values of applied field (up to about 12 kOe) and for different fixed values of entropy. (Alternatively, this may be viewed as beginning at different initial temperatures for a given magnitude and direction of field. In Fig. 13 we show results for two different rotation experiments: $H_0 = 4.0$ kOe and $S/R \sim 0.185$, and $H_0 = 12.2$ kOe and $S/R \sim 0.054$. (Note the change in scale between the upper and lower portions of Fig. 13). Examination of the phase diagrams shown earlier suggests that during the low-field rotation the sample remained in the simple antiferromagnetic state, but the high-field rotation enters both the paramagnetic state and the "multiaxis" states near [110] and [001].

D. Multiaxis-susceptibility measurements

We have described the phase diagrams and have indicated proposed spin arrangements for all phases with fields in the three principal directions. The most desirable method of checking these predictions would be neutron diffraction but this is not possible to do with the facilities in our laboratory. The only means of obtaining information concerning the magnetic state of the system is by making measurements of the susceptibility with a large static field, H_0 , perpendicular to the ac measuring field h . Unfortunately our apparatus does not exclude temperature-in-

dependent "background" contributions. However, the zero-field susceptibility is well known,¹ and by comparing with a zero-field measurement on our apparatus, we may determine the size of our susceptibility "units" on absolute scale, provided the same current and frequency are used for all subsequent measurements. The mere presence of the magnet changes the zero dramatically as does the subsequent application of a field. The only tenable solution to this problem is to normalize the results with the zero-field curve at 4.2 K. In DyAlG the Weiss Θ is determined by spins which are *parallel* to those being measured. Because the large applied field constrains only those spins perpendicular to those being measured by the measuring field, the Weiss Θ is unchanged due to the application of the field. Thus only the terms of second order and higher in interactions will be different in zero field and with fields parallel to [001] and [110]. To a good approximation the zero-field susceptibility obeys a Curie-Weiss law at 4.2 K. (This clearly is not exact, but it does provide a reasonable estimate for the true absolute scale.) The results of susceptibility measurements are shown in Fig. 14 for: (i) zero field (χ is isotropic), (ii) $\bar{h} \parallel [110]$, $\bar{H}_0 \parallel [001]$, and (iii) $\bar{h} \parallel [001]$, $\bar{H}_0 \parallel [110]$, where H_0 is the large static field and h the ac measuring field. The results have been corrected to a spherical specimen using the relation

$$\chi_{\text{sphere}}^{-1} = \chi_{\text{exp}}^{-1} + \left(\frac{1}{3}4\pi - N_{\text{exp}}\right). \quad (11)$$

The data in Fig. 14 show unambiguously that the ordered state for $\bar{H}_0 \parallel [001]$ is antiferromagnetic. The susceptibility has a maximum about 15% above the ordering temperature and decreases as the temperature is lowered. Within experimental error the maximum slope of χT coincides with the ordering temperature.

The interpretation of the results for $\bar{H}_0 \parallel [110]$ and $\bar{h} \parallel [001]$ is more difficult. At first glance the behavior seems to indicate antiferromagnetic order; however, χ_{max} is very close to $1/N$, which would be the maximum for a ferromagnetic state. In addition the transition temperature coincides more closely with the maximum in χ than the maximum slope of χT . Both of these facts would suggest ferromagnetic ordering.³¹ Very recent preliminary neutron scattering experiments²⁹ show that the alternative structures which appear possible based on the dipolar interactions¹¹ are *not* consistent with the neutron data. In addition, measurements of the magnetic moment with strong fields applied near a [110] axis indicate that the long-range order is ferromagnetic.³² This is consistent with the results given here, and we therefore conclude that the low-temperature high-field state is ferromagnetic (i.e., P_m, P_m, F).

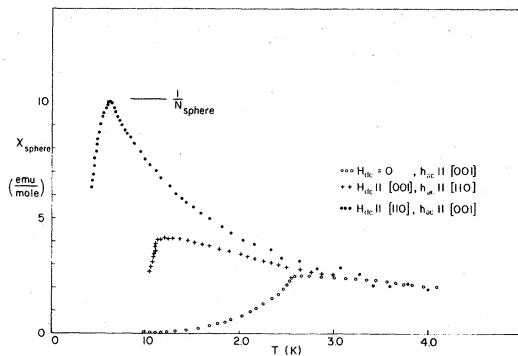


FIG. 14. Susceptibility of DyAlG with large static-magnetic fields along [110] and [001] (ac measuring perpendicular to the large field and in zero field.) The results have been corrected to a spherical sample with $N = \frac{1}{3}4\pi$.

V. ANALYSIS AND DISCUSSION

A. Phase diagrams

1. Low-field boundaries

The behavior of the critical field as $T \rightarrow T_N$ (i.e., $H^c \rightarrow 0$) has been examined for the three principal directions: [110], [001], and [111]. The intrinsic quantity of interest is the internal field H_i^c and in order to correct our results at constant external field H_0 we used the magnetization data of Wyatt.²⁴ The critical field H_i^c is expected to behave as

$$H_i^c = A(1 - T/T_N)^{1/2} \quad (12)$$

as $T \rightarrow T_N$. The data were therefore analyzed by plotting H_i^c (Ref. 2) vs $T_N - T$. The results for [110] and [001] are plotted in Fig. 15. For comparison we also show the variation of the "ghost" of the transition²³ which appears when the applied field is along [111]. The data are consistent with Eq. (12) with a single value of $A = 6.6 \pm 0.1$ kOe, independent of direction. The observed tricritical temperatures in the [001] and [110] directions are also almost identical, and we estimate that the location of the tricritical point in the [111] direction would also be quite similar if it were experimentally accessible. Bidaux *et al.*¹⁴ have explained this behavior using the molecular-field theory; the close agreement in the three directions is fortuitous.

2. Low-temperature high-field transitions

There are a number of interesting features associated with the high-field transitions between the partially aligned paramagnetic state and the "multiaxis" phases. With the field along, or near, [001] the phase boundary bends back in temperature as the field increases. This can be understood primarily in terms of the misalignment of the field which introduces a com-

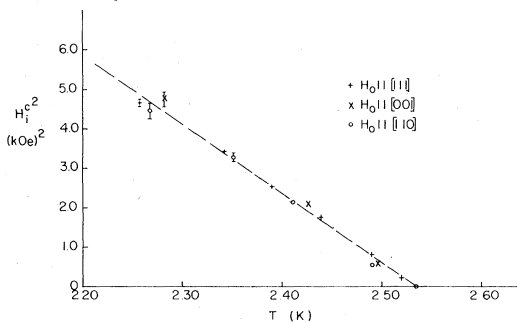


FIG. 15. Behavior of the critical field as $T \rightarrow T_N$ for fields in the three principal directions.

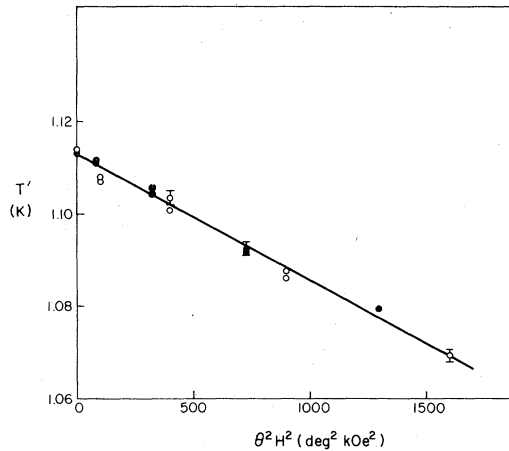


FIG. 16. Variation of transition temperature with misalignment angle θ for fields near [001] in DyAlG. The linear dependence of $T'_{[001]}$ vs θ^2 shows $T'_{[001]} \propto H^2$ for small angles. For $\theta=0$, H_0 is along [110].

ponent $H_1 = H_0 \sin\theta$ along the [110] direction where θ is the angular misorientation from [001]. This component lowers the transition temperature of the transverse antiferromagnetic sublattices of the (A_2, A_2, P_m) phase. The effect is to trace out a critical-field curve analogous to the one for the (A_1, A_1, A_1) phase. For fields not substantially greater than $H_0=7$ kOe we expect [in analogy with Eq. (12)],

$$H_1 = H_0 \sin\theta = A_1(1 - T'/T_{[001]}^\perp)^{1/2}, \quad (13)$$

where $T_{[001]}^\perp$ is the ordering temperature for $\theta=0$, and T' is the transition temperature for a misalignment by θ . For small misalignment we have $\sin\theta \sim \theta$ and Eq. (13) becomes

$$\theta^2 H_0^2 = A_1^2 / T_{[001]}^\perp (T_{[001]}^\perp - T'). \quad (14)$$

The data for $H_0=9$ kOe and 10 kOe shown in Fig. 6 are analyzed in Fig. 16. (The data should show symmetry for misalignment about [001] since [110] and $[\bar{1}\bar{1}0]$ are equivalent. The best fit occurs when the magnet vernier reading of 4° is taken as perfect [001] alignment.) The data show the behavior predicted by Eq. (14) with $T_{[001]}^\perp = 1.113 \pm 0.005$ K and support the critical-field interpretation given above. Even when the field was completely aligned (to within an estimated $\pm \frac{1}{2}^\circ$) the vertical phase boundary continued to bend back for $H_0 \geq 10$ kOe. We believe that this is due in large part to the small (but nonzero) g_\perp .

One particularly fascinating feature of this phase boundary is the negative specific heat which occurred at high fields when the alignment was not perfect. We believe this is a real effect which results from the unusual multisublattice nature of DyAlG, the storage of energy in the twisted sample support and the rela-

tive slowness of heat flow. (It is also quite possible that irreversible effects enter.) Because the magnetocrystalline anisotropy constrains the sublattice moments to lie in [001] directions, the sample magnetization will not generally be parallel to the applied field, and the sample will experience a torque. Simple mean-field calculations suffice to show that in the paramagnetic state only the [111] direction represents a direction of stable equilibrium. Both [001] and [110] are directions of unstable equilibrium: the torque is zero if the applied field is exactly along one of these directions, but is nonzero for small misalignment and tends to rotate the sample towards [111]. With $T = 0.8$ K and $H_0 = 10$ kOe, torques as large as 5×10^6 dyne cm can be produced.^{19,33} At low temperatures and large fields near [001], the (A_2, A_2, P_m) is realized and the [001] direction also becomes stable. As the sample is heated through the transition temperature T' , the antiferromagnetically ordered transverse spins become paramagnetic. Since it is also quite possible that a tricritical line appears for the transverse phase [i.e., the $(A_2, A_2, P_m) \rightarrow (P_d, P_d, P_m)$ transition becomes first order] the conversion of one phase to another is "driven" by the heat. The conversion to the paramagnetic state once again makes [001] an unstable direction and the sample rotates. When this occurs, energy is stored in the twisted support and the sample cools due to the negative sign of the magnetocaloric effect (note the cooling observed in the adiabatic rotation shown in Fig. 13 as the field is rotated away from [001]).

The high-field phase boundary for H_0 along [110] is virtually field independent above 8 kOe. The data shown in Fig. 11 indicate the multisublattice behavior with the peak at $T_{[011]}^1 \sim 0.6$ K due to the $(P_m, P_m, F) \rightarrow (P_m, P_m, P_d)$ transition clearly separated from the rounded Schottky maximum due to the paramagnetic spins, which are aligned by the field. A simple attempt to separate out the contributions from the spins aligned by the field can be made by calculating a Schottky peak due to energy gap $\Delta = g\mu_B H$ with $H = H_0 + h_{\text{int}}$, where h_{int} is the interaction field produced by the aligned spins. The characteristic form for this curve [Eq. (4)] is multiplied by $\frac{2}{3}$ since only $\frac{2}{3}$ of the spins are involved and is plotted along with the experimental data in Fig. 11. Since this curve exceeds the total measured specific heat, the neglect of interactions with transverse (disordered) spins is serious. The effect of these interactions may be included in a relatively crude fashion through calculation of the modified Schottky curve determined in the following way: Since the transverse spins are disordered, their relative direction (and hence interaction) with respect to the "parallel" (aligned paramagnetic) spins varies from site to site. It is straightforward to show that, because of symmetry, at about 50% of the parallel sites the interaction due to

nearest-neighbor transverse spins cancels out (see Fig. 3). Conversely at one quarter of the sites they add a contribution to the gap of Δ' and at the remaining sites add a contribution $-\Delta'$. The "modified" Schottky curve shown in Fig. 11 is simply the sum of three Schottky curves with $\Delta = g\mu_B H + \Delta'$, $\Delta = g\mu_B H$, and $\Delta = g\mu_B H - \Delta'$ weighted by $\frac{1}{4}$, $\frac{1}{2}$, and $\frac{1}{4}$, respectively. This approximation should in fact be quite good as long as the Schottky specific heat is small. At higher temperatures where multiple excitations of the parallel spins become important, the modified Schottky should offer less improvement over the simple Schottky.

3. Magnetic phase boundaries in the (110) plane

The phase boundaries of DyAlG with fields along the principal axes have been studied using mean-field theory.^{5,11,15} However, these studies as well as the experimental investigations of Bidaux *et al.*³² have been restricted to low temperatures. The extent and nature of the multisublattice behavior can best be understood from a diagram which shows phase boundaries as a function of *both* field orientation *and* temperature. Using our results and those of Bidaux *et al.*,³² we have constructed such a three-dimensional plot for internal fields H_i in Fig. 17(a). In this figure the stipled surfaces represent the phase boundaries. The (P_m, P_m, F) state is seen to exist only in the [110]- T plane, whereas (A_2, A_2, P_m) exists in a three-dimensional volume near [001]. The letters A-F represent special points on the diagram and will be useful in interpreting the phase diagram for external fields H_0 shown in Fig. 17(b). Because of the existence of the demagnetizing field, all first-order transitions are spread out over a range of external field. For example point E in Fig. 17(a) becomes a line $E-E'$ in Fig. 17(b). The effect of the demagnetizing field on points B and C is even more severe and they are spread out into the *surfaces* $B-B'-B''$ and $C-C'-C''$, respectively. Obviously experiments carried out in any single plane (e.g., constant T or constant field direction) may show very complicated behavior due to demagnetizing field effects, even though the underlying intrinsic behavior (i.e., H_i-T) is relatively simple. As an example the reader is urged to compare the phase diagrams in Figs. 5 and 10 with Figs. 17(a) and 17(b).

B. Extraction of characteristic parameters

1. Determination of the critical fields as $T \rightarrow 0$ K

In the molecular-field theory the critical field at absolute zero is determined by the difference in interac-

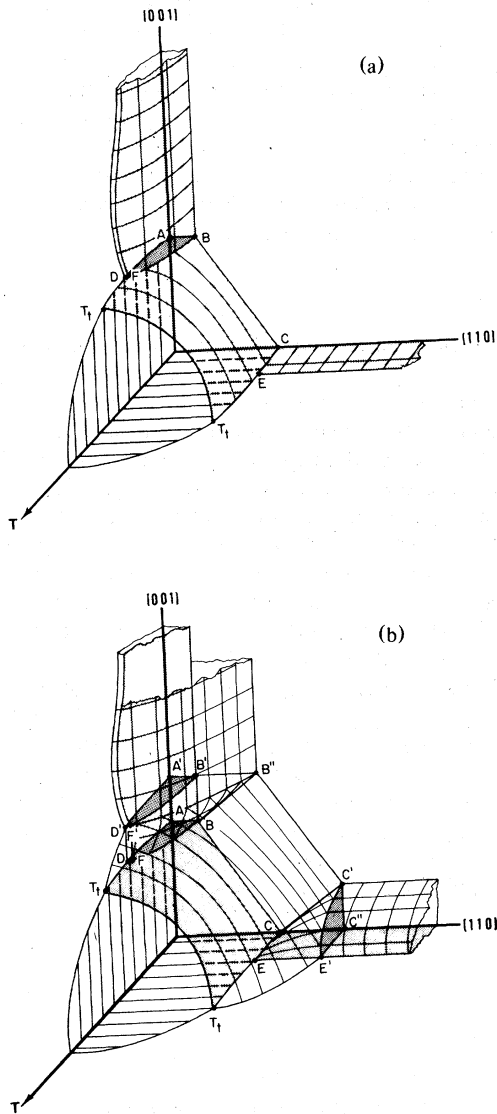


FIG. 17. Magnetic phase diagram for DyAlG as a function of temperature for applied magnetic fields in the (110) plane (this figure shows a 90° range of field orientation from [110] to [001]): (a) as a function of H_i . Here the surfaces depicted by the grainy surface and by the thin contour lines coincide. (b) as a function of applied magnetic field H_0 with $N = 5.35$. Here the effect of the nonzero demagnetizing factor is to cause the surface indicated by the contour lines to separate from those depicted by the grain. This results from the fact that the passage between phases proceeds via a first-order phase transition. Thus all points labeled with the same letter (e.g., B, B', B'') coalesce in the plot as a function of internal field. By taking cross sections in the [110]- T , [111]- T , and [001]- T planes, one obtains the H_0 vs T magnetic phase diagrams shown earlier (see Figs. 5 and 10 and Ref. 3). The location of the conjectured line of tricritical points ending in point F is approximate.

tion energy between the perfectly ordered and disordered states, and can be used to yield information about the spin-spin interactions. We have seen that, because our sample has a finite demagnetizing factor, the transition will occur over a range of external field delineated by H_0^+ and H_0^- , i.e., the upper and lower boundaries. They are related to the actual internal critical field for $T=0$ by

$$H^- = H_0^-, \quad H^+ = H_0^+ - NM_0, \quad (15)$$

where M_0 is the saturation magnetization and where the two estimates for H_i^c should be identical at $T=0$ K. In fact they are not, due only, we believe, to experimental error. These errors include the difficulty in interpreting the latent-heat curves, measuring the field, and determining the saturation magnetization. In addition our experiments were done at relatively high temperatures and the critical field is still changing with temperature. Figures 18 and 19 show plots of H_0^- and $H_0^+ - NM_0$, where M_0 is 545 and 385 Oe for [110] and [001] directions, respectively. From these we have estimated the critical fields

$$H_{[110]}^i = 4700 \pm 80 \text{ Oe}, \quad H_{[001]}^i = 5150 \pm 100 \text{ Oe}.$$

The H^- 's were weighed more heavily because of the possible error in M_0 which must be used to correct H^+ . These curves also indicate that $\partial H_i^c / \partial T$ is very small as $T \rightarrow 0$ and probably zero.

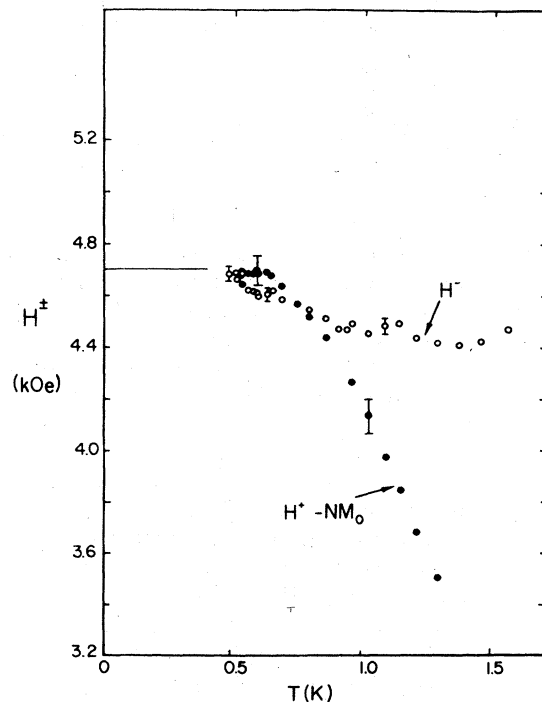


FIG. 18. Extrapolation of low-temperature critical field to $T=0$ K for DyAlG with fields along [110].

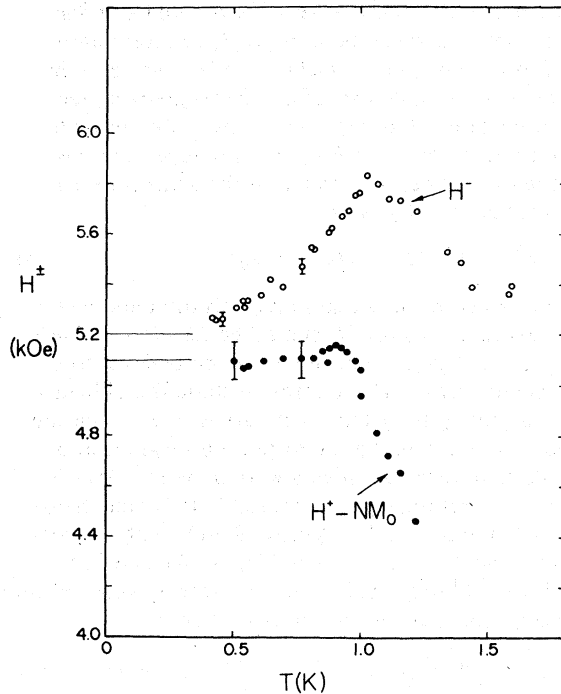


FIG. 19. Extrapolation of low-temperature critical field to $T = 0$ K for DyAlG with fields along [001].

The effect of misaligning strong fields with respect to the [001] direction is to put a small applied field along the high g direction of the transverse spins. As described earlier, they will react just as any antifer-

$$\frac{C}{R} = \frac{2}{3} \left(\frac{\Delta_{[001]}}{T} \right)^2 \exp \left(-\frac{\Delta_{[001]}}{T} \right) + \frac{1}{3} \left(\frac{\Delta'}{T} \right)^2 \exp \left(-\frac{\Delta'}{T} \right), \quad (16)$$

where $\Delta_{[001]}$ is the gap for the transverse spins and $\Delta' = g \mu_B (H_0 + h_{\text{int}})$ with a small interaction field h_{int} between z spins. Runs were made down to 0.5 K for two different values of the applied field, 8.55 and 12.27 kOe. For both cases $\Delta' \geq 10$ K and the contribution of the second term in Eq. (15) is negligible below 0.8 K. Because of the misalignment of the applied field, the transverse antiferromagnetically aligned spins see a small component of applied field and the up and down spins have different energy gaps. It can be shown that to lowest order in the field and interactions the low-temperature specific heat is then given by Eq. (3) where $\delta = g \mu_B H_0 \sin \theta$. By fitting the low-temperature data to Eq. (3) we were able to deduce that the field had been misaligned by $\sim 2.1^\circ$. The data were corrected for misalignment and then fitted to the asymptotic low-temperature behavior given by Eq. (16) using an effective value of Δ . (This procedure was described

romagnet in a small field, and a critical-field curve will result. The critical field $(H_c^{\pm})_{[001]}$ as $T \rightarrow 0$ K which would be necessary to cause the transverse spins to become paramagnetic [i.e., the transition between (A_2, A_2, P_m) and (P_m, P_m, P_m)] can be obtained from Ref. 32 and is $(H_c^{\pm})_{[001]} = 1.05 \pm 0.05$ kOe. Because the transverse spin state with H_0 along [110] is ferromagnetic, there is no equivalent critical-field curve for the transverse spins.

2. Determination of the low-temperature energy gaps

In a highly anisotropic system like DyAlG the low-temperature elementary excitations are single ion "spin flips" rather than collective modes. The low-temperature specific heat is therefore expected to asymptotically have the form shown in Eq. (2), as $T \rightarrow 0$ where Δ is the energy gap for excitations, i.e., the energy required to overturn a single spin in the ordered state. With strong fields along either [001] or [110] we expect the low-temperature specific heat to have two contributions of this form: those spins which are "parallel" to the applied field will have a very large energy gap due essentially to the Zeeman splitting and the contribution at low temperatures will be quite small. The ordered transverse spin states will have smaller energy gaps determined by the interactions between the transverse spins. Therefore, for an applied field along the [001] direction the low-temperature specific heat should have the form

in detail in Ref. 3 where the low-temperature zero-field behavior was analyzed). The temperature variation of this effective Δ is shown in Fig. 20. This vari-

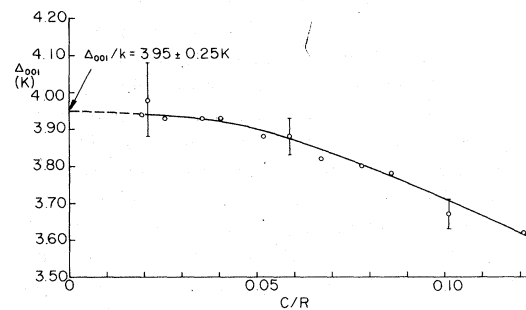


FIG. 20. Determination of low-temperature energy gap $\Delta_{[001]}$ for DyAlG with large fields along [001].

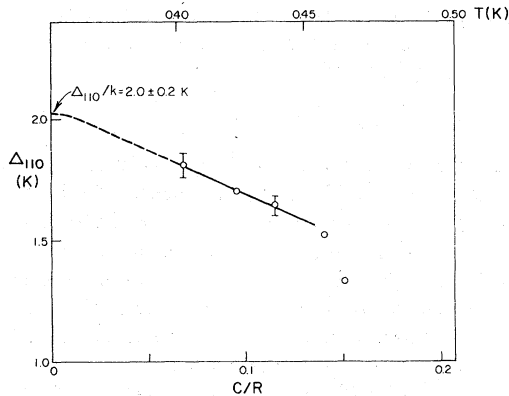


FIG. 21. Determination of the low-temperature energy gap $\Delta_{[110]}$ for DyAlG with large fields along [110].

ation suggests a value of $\Delta_{[001]}/k = 3.95 \pm 0.25$ K where the major portion of the error comes from the uncertainty in the misalignment.

With the field along [110] it would be necessary to go to very low temperatures (~ 0.3 K) in order to determine $\Delta_{[110]}(0)$ as accurately as $\Delta_{[001]}$; this was not possible with our experimental apparatus,³⁴ and we can only make a less precise estimate from higher-temperature data. Note that because the results in different fields are almost identical (as shown in Fig. 11), it appears that the correction for misalignment is very small in this direction. The analysis of the low-temperature specific-heat data with 11.65 kOe along the [110] direction is shown in Fig. 21. From this graph we extrapolate the data in a manner consistent with Fig. 20 to estimate $\Delta_{[110]}(0) = 2.0 \pm 0.2$ K.

3. High-temperature specific-heat coefficients

At sufficiently high temperatures compared to the magnetic interactions, the specific heat asymptotically approaches the characteristic form⁴ given by Eq. (7). Once again for the cases we are considering now, there are actually two magnetic systems, one composed of the spins which have a component of the field along their high- g axes and another including those which are perpendicular to the field. The specific heat resulting from the first kind of spins will produce a rounded Schottky curve, and the specific heat of the spins which are perpendicular to the field is superimposed on the Schottky anomaly [at high temperatures adding a contribution of the form given in Eq. (7)]. For fields of the order of 10 kOe along either [110] or [001] the Schottky anomaly will appear at a higher temperature than the peaks due to ordering of the transverse spins. Since both g_z and h_i were determined previously,⁴ we calculated the Schottky specific heat using the modified Schottky method described earlier, and subtracted it from the total measured specific heat yielding a net specific

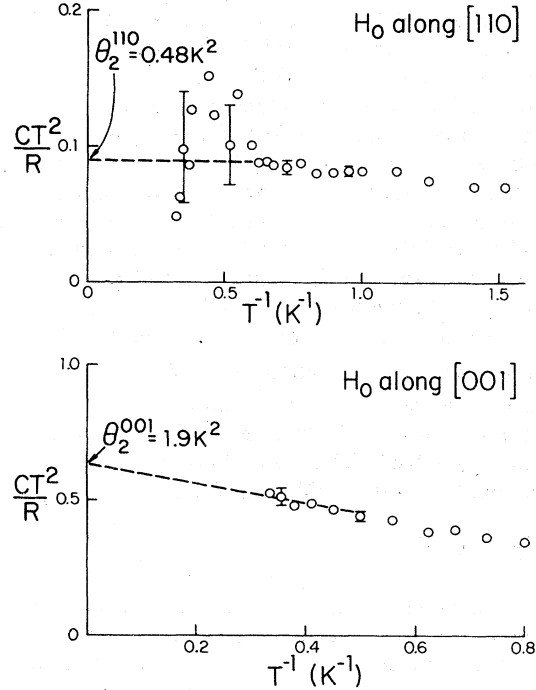


FIG. 22. Above: analysis of high-temperature specific heat with H_0 along [110]; below: analysis of high-temperature specific heat with H_0 along [001].

heat C'/R for the spins perpendicular to the field. (For $H_0 = 14.73$ kOe along [110] the Schottky comprised 1% of the total at 1 K but 60% at 2 K. With $H_0 = 14.73$ kOe along [001] the Schottky contribution was 4% at 2 K and nearly 31% at 3 K.) From the plots of $C'T^2/R$ vs T^{-1} we have determined the asymptotic forms of the specific heat (see Fig. 22),

$$\Theta_2^{[001]} = 1.9 \pm 0.6 \text{ K}^2, \quad \Theta_3^{[001]} = -1.4 \pm 1.0 \text{ K}^3;$$

$$\Theta_2^{[110]} = 0.48 \pm 0.20 \text{ K}^2, \quad \Theta_3^{[110]} = 0.0 \pm 0.20 \text{ K}^3.$$

4. Thermodynamic functions for the "multiaxis" transitions

In Sec. V B 3 we saw that the "zero-field" transitions of the spins perpendicular to the magnetic field were quite similar to the true zero-field transition $(A_1, A_1, A_1) \rightarrow (P_d, P_d, P_d)$. From the results for $\bar{H}_0 (= 8.55 \text{ kOe}) \parallel [001]$, we have been able to determine the characteristics of the entropy and internal energy associated with the transition of the $\pm X, \pm Y$ spins to the antiferromagnetic state. The entropy is determined from the specific heat from the relation

$$\frac{S}{R} = \int_{T_1}^{T_2} \frac{C}{RT} dT. \quad (17)$$

The entropy associated with the measured specific

heat was $(0.361 \pm 0.007)R$. Using the low-temperature form determined earlier, we found $S/R = 0.003 \pm 0.001$ ($T < 0.5$ K). The extrapolation at higher temperatures was rather more difficult. Above 1 K the specific heat from the spins aligned by the field became significant and the data were corrected for the contribution using the values for Θ_2, Θ_3 obtained in Sec. V B 3. We obtained $S/R = 0.063 \pm 0.015$ ($T > 1.5$ K). The total entropy with this transition is $(0.46 \pm 0.028)R$ or about $0.670R \ln 2$. The temperature variation of the entropy is shown in Fig. 23. (If exactly $\frac{2}{3}$ of the spins were involved in the transition, $\frac{2}{3}R \ln 2$ entropy should be involved.) The critical entropy, $(S_c - S_0)/R$, is 0.268 ± 0.008 or about 58% of the total entropy involved. The internal energy can be determined from the specific heat from

$$\frac{U}{R} = \int_{T_1}^{T_2} \frac{C}{R} dT, \quad (18)$$

where we have taken the zero of the internal energy to be at $T = \infty$. [Eq. (18) is valid since the portion of the system under consideration is perpendicular to the field it is essentially in a zero-field state.] Using the low-temperature extrapolation, we find $U/R = 0.002$ ($T < 0.5$ K). In the region actually measured $U/R = 0.401 \pm 0.008$ and using the same high-temperature extrapolation of the specific heat as we did for the entropy, we find $U/R = 0.273 \pm 0.040$ ($T > 2.0$ K). The large error in the determination of this quantity arises from the uncertainty in the extrapolation of the high-temperature specific heat and will therefore introduce a large error into the determination of the internal energy. The total energy is then $U/R = 0.702 \pm 0.050$. Remembering that only $\frac{2}{3}$ of a

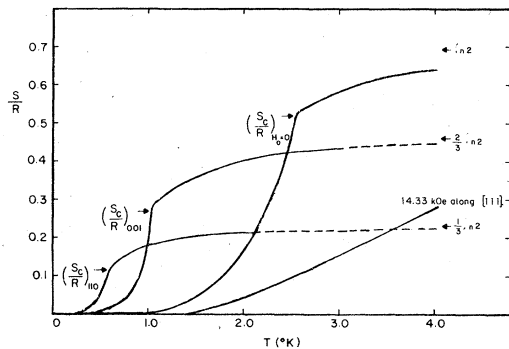


FIG. 23. Entropy vs Temperature for the case H_0 along [110], [001]. These show the entropy characteristics for the transverse-ordered states. The solid lines show actual experimental values corrected for the contribution of the spins aligned by the field. The dashed lines indicate the extrapolated curve for the transverse spins along. The zero-field curve is shown for comparison as is the result for a large field along [111].

mole of spins were involved, we can use the relation⁴ between the low-temperature energy gap and the internal energy to estimate

$$\Delta_{[001]}/k = 4(U/R) = 4.2 \pm 0.4 \text{ K}.$$

This is in good agreement with the value of $\Delta_{[001]}(0) = 3.95 \pm 0.25$ K obtained directly from the low-temperature specific heat. In view of the substantial errors the agreement is quite satisfying.

For $\vec{H}_0 \parallel [110]$ the above analysis will be even less accurate than in the [001] case because of the relative lack of low-temperature data. From extrapolation to $T = 0$ K and $T = \infty$, we obtain a total $S/R = 0.226 \pm 0.028$ and $(S_c - S_0)/R = 0.115 \pm 0.022$ or about 51% of the total (see Fig. 23). (If exactly $\frac{1}{3}$ of the spins were involved in the transition, the total energy was found to be $U/R = 0.201 \pm 0.025$), and the low-temperature energy gap determined from the internal energy was $\Delta_{[110]}/k = 2.4 \pm 0.3$ K. From the low-temperature specific heat we obtained the value $\Delta_{[110]}/k = 2.0 \pm 0.2$ K. The agreement is certainly adequate. It should be noted that for both the [110] and [001] directions the total calculated entropy is greater than the allowable total, $\frac{1}{3}R \ln 2$ and $\frac{2}{3}R \ln 2$, respectively, and indicates that the values obtained for U/R and thus $\Delta(0)$ are also too high.

We can obtain a measure of confidence in our low-temperature entropy determination from the results of the adiabatic-field rotation shown in Fig. 13. With the field in the [111] direction $T = 1.88$ K, the entropy was known fairly well to be $S/R = 0.054$ (see Ref. 35). With the field rotated into the [001] and [110] directions, the temperature fell to 0.82 and 0.51 K, respectively. From the entropy-temperature relationships determined above, we find that these temperatures correspond to $S/R = 0.053$ for $\vec{H}_0 \parallel [110]$ and 0.052 for $\vec{H}_0 \parallel [001]$ (see Fig. 23). The close agreement with the [110] case is particularly important because it indicates that our low-temperature extrapolation was probably rather accurate, and any errors in the entropy are probably due to the high-temperature extrapolation.

VI. SUMMARY

A series of magnetothermal experiments on DyAlG have demonstrated the existence of order-order and order-disorder transitions involving noncollinear sublattices. Phase diagrams have now been determined experimentally for magnetic fields in the [111], [110], and [001] directions.³ (About 100 points were included in each phase diagram between 0.5 and 2.54 K.) For $\vec{H}_0 \parallel [001]$, [110] the transitions from the simple antiferromagnetic state to the paramagnetic state were higher than first order above 1.66 K, and were of first order below 1.66 K.

TABLE I. Characteristic parameters with fields along [110], [001].

| | |
|----------------------------|----------------------------------------------------|
| $H_{[110]}^c(0)$ | 4700 ± 80 Oe 4700 Oe ^b |
| $H_{[001]}^c(0)$ | 5150 ± 100 Oe 5140 ± 50 Oe ^a |
| $[H_{\perp}^c(0)]_{[001]}$ | 1050 ± 50 Oe ^b |
| $\Delta_{[001]}/k$ | 3.95 ± 0.25 K |
| $\Delta_{[110]}/k$ | 2.00 ± 0.20 K |
| $(T_c)_{[001]}$ | 1.65 ± 0.01 K ^c |
| $(T_c)_{[110]}$ | 1.71 ± 0.02 K ^c |
| $\theta_2^{[001]}$ | 1.9 ± 0.6 K ² |
| $\theta_2^{[110]}$ | 0.48 ± 0.20 K ² |
| $(S_c/R)_{[001]}$ | 0.268 ± 0.008 |
| $(S_c/R)_{[110]}$ | 0.115 ± 0.022 |
| $(U/R)_{[001]}$ | 0.70 ± 0.05 |
| $(U/R)_{[110]}$ | 0.20 ± 0.025 |
| $T_{[001]}^{\perp}$ | 1.1 ± 0.1 K |
| $T_{[110]}^{\perp}$ | 0.61 ± 0.02 K |
| $\theta_3^{[001]}$ | -1.4 ± 1.0 K ³ |
| $\theta_3^{[110]}$ | 0.0 ± 0.2 K ³ |

^aReference 32.

^bEstimates were obtained from the figures in Reference 32.

^cError limits apply to present measurements. Effects of misalignment are not included.

The latent heats were measured directly for all three directions by isothermal-field sweeps; for $\vec{H}_0 \parallel [001]$ the latent heat became negative indicating $\partial H^c/\partial T$

was positive. At 0.5 K and below, the latent heat was very small in all cases indicating that $\partial H^c/\partial T$ was essentially zero in all three cases and might in fact be zero at $T \rightarrow 0$ K. We wish to note that such asymptotic behavior is not mandatory. A recent Monte Carlo study³⁶ on a bcc Ising antiferromagnet yielded a nonzero asymptotic value of $\partial H^c/\partial T$. This behavior is not inconsistent with the present result for DyAlG, since the model included only nearest-neighbor coupling and the phase boundary remained second order down to $T = 0$.

The transition from high-field low-temperature states (for $\vec{H}_0 \parallel [110], [001]$) to the paramagnetic state was marked by a λ -type specific-heat peak, which was unusually sharp. The low-temperature energy gaps were measured, and the critical fields $H^c(T)$ were measured and extrapolated to 0 K. Therefore, we conclude that we have observed multiaxis cooperative transitions and find that to a good approximation the spins which are not aligned by the field form a relatively free system with characteristic parameters such as low-temperature energy gap, ordering temperature, and critical-field curve (see Table I). In the following paper in this series we shall use these characteristic parameters to determine the spin-spin interaction parameters.

ACKNOWLEDGMENTS

We wish to thank R. Alben, M. Blume, N. Giordano, R. B. Griffiths, and J. E. Rives for helpful discussions and comments. We would particularly like to acknowledge Professor W. P. Wolf for his involvement in the initial phases of analysis and for his constant advice and encouragement. Portions of this research were supported by the AEC and by the NSF.

*Present address: Dept of Phys. and Astron., University of Georgia, Athens, Ga. 30602.

†Present address: Atomic Energy Research Establishment, Harwell, Didcot, Berks, England.

¹M. Ball, M. T. Hutchings, M. J. M. Leask, and W. P. Wolf, *Proceedings of the Eighth International Conference on Low Temperature Physics*, edited by R. O. Davies (Butterworths, London, 1963).

²J. M. Hastings, L. M. Corliss, and C. G. Windsor, *Phys. Rev. A* **138**, 176 (1965).

³D. P. Landau, B. E. Keen, B. Schneider, and W. P. Wolf, *Phys. Rev. B* **3**, 2310 (1971).

⁴W. P. Wolf, B. Schneider, D. P. Landau, and B. E. Keen, *Phys. Rev. B* **5**, 4472 (1972).

⁵R. Alben, M. Blume, L. M. Corliss, and J. M. Hastings, *Phys. Rev. B* **11**, 295 (1975).

⁶J. F. Dillon, Jr., E. Y. Chen, and W. P. Wolf, *Proceedings of the 9th International Conference on Magnetism, Moscow, 1973* (Nauka, Moscow, 1974); J. F. Dillon, Jr., E. Y. Chen, and W. P. Wolf, *AIP Conf. Proc.* **18**, 334 (1974); J. F. Dillon, Jr., E. Y. Chen, N. Giordano, and W. P. Wolf, *Phys. Rev. Lett.* **33**, 98 (1974).

⁷R. B. Griffiths, *Phys. Rev. Lett.* **24**, 715 (1970).

⁸B. E. Keen, D. P. Landau, and W. P. Wolf, *Phys. Lett.* **23**, 202 (1966).

⁹K. Motizuki, *J. Phys. Soc. Jpn.* **14**, 759 (1959).

¹⁰W. E. Gardner and N. Kurti, *Proc. R. Soc. London A* **223**, 543 (1954).

¹¹D. P. Landau, thesis (Yale University, 1967) (unpublished).

¹²W. P. Wolf, B. E. Keen, D. P. Landau, and B. Schneider, *Proceedings of the Tenth International Conference on Low Temperature Physics, Moscow (1966)*, edited by M. P. Mal-

- kov (VINITI, Moscow, 1967), Vol. 4, p. 136.
- ¹³A. H. Cooke, D. T. Edmonds, C. B. P. Finn, and W. P. Wolf, Proc. R. Soc. London 306, 335 (1968).
- ¹⁴R. Bidaux, P. Carrara, and B. Vivet, Phys. Lett. A 25, 322 (1967).
- ¹⁵R. Bidaux and B. Vivet, J. Phys. (Paris) 29, 57 (1968).
- ¹⁶R. Bidaux, P. Carrara, and B. Vivet, J. Phys. (Paris) 28, 187 (1967).
- ¹⁷A full account of the various possible states will be given in the last paper to be published. See also Ref. 19.
- ¹⁸A. F. Wakefield, Proc. Cambridge Philos. Soc. 47, 419 (1951).
- ¹⁹W. P. Wolf, *Proceeding of the 6th International Conference on Magnetism* (Institute of Physics and Physical Society, London, 1964), p. 555.
- ²⁰J. F. Cochran, C. A. Schiffman, and J. E. Neighbor, Rev. Sci. Instrum. 37, 499 (1966).
- ²¹G. S. Dixon and J. E. Rives, Phys. Rev. 177, 871 (1969).
- ²²F. R. McKim and W. P. Wolf, J. Sci. Instrum. 34, 64 (1957).
- ²³Similar sharp peaks were observed with $\vec{H}_0 \parallel [111]$ (see Ref. 3). In Refs. 3 and 4 it had been assumed that these peaks signaled the phase transition $(A_1, A_1, A_1) \rightarrow (P_m, P_m, P_m)$. As described in the Introduction, we now believe that the application of an applied field simultaneously produces a very small staggered field. The specific-heat measurements therefore never actually passed through the phase boundary but merely nearby. For $\vec{H}_0 \parallel [110]$ and $\vec{H}_0 \parallel [001]$ the staggered field effect is absent and the measured specific-heat peaks actually indicate the location of the phase boundary.
- ²⁴A. F. G. Wyatt, thesis (Oxford University, 1963) (unpublished).
- ²⁵P. M. Levy, Phys. Rev. 170, 595 (1968); P. M. Levy and D. P. Landau, J. Appl. Phys. 39, 1128 (1968).
- ²⁶N. Giordano and W. P. Wolf, AIP Conf. Proc. 29, 459 (1976); N. Giordano and W. P. Wolf, Phys. Rev. Lett. 35, 799 (1975).
- ²⁷This effect is explained by mean-field theory in Ref. 32.
- ²⁸Although the change in order of the transition occurs at a "wing" critical point when $\vec{H}_0 \parallel [111]$, the magnitude of the effective staggered field is expected to be quite small (~ 1 Oe) (see Ref. 26) and the tricritical temperature should not be very different from the observed "wing" critical temperature.
- ²⁹M. Steiner and N. Giordano, J. Phys. (Paris) 39, C6-810 (1978); and unpublished.
- ³⁰B. E. Keen and D. P. Landau (unpublished).
- ³¹Both a maximum in the inductive component of the susceptibility at the critical temperature and a growth of the resistive component below the critical temperature have been observed in ferromagnetic dysprosium ethyl sulfate, (see Ref. 13).
- ³²R. Bidaux, P. Carrara, and B. Vivet, J. Phys. 29, 357 (1968).
- ³³B. A. Calhoun and W. P. Wolf, Bull. Am. Phys. Soc. 11, 254 (1966).
- ³⁴A difficulty here was that it was not only necessary to cool through the cooperative anomaly at 0.6 K, but it was necessary to remove the entropy associated with the Schottky peak due to the application of the field along [110].
- ³⁵If the field was aligned perfectly along [001] and g_x, g_y were identically zero, this state would be (P_m, P_m, P_d) .
- ³⁶D. P. Landau, Phys. Rev. B 16, 4164 (1977).